Surface and Internal Spin Canting in γ-Fe_2O_3 Nanoparticles

M. P. Morales,* S. Veintemillas-Verdaguer, M. I. Montero, and C. J. Serna

Instituto de Ciencia de Materiales de Madrid, CSIC, Cantoblanco, 28049 Madrid, Spain

A. Roig, Ll. Casas, B. Martínez, and F. Sandiumenge

Instituto de Ciencia de Materiales de Barcelona, CSIC, Campus UAB, 08193 Bellaterra, Barcelona, Spain

Received February 11, 1999. Revised Manuscript Received August 9, 1999

Structural and magnetic properties of γ-Fe_2O_3 have been studied in isometric nanoparticles ranging from 3 to 14 nm with a narrow particle size distribution. Cation vacancy order is observed for particles larger than 5 nm in diameter giving rise to a cubic superstructure, while for the smallest particles these vacancies are disordered. All magnetic properties measured showed a strong dependence on the average crystallite size. For the ordered samples, saturation magnetization was found to decrease linearly with decreasing crystallite size due to a surface spin canting effect. However, a stronger decrease was observed in the disordered samples, suggesting that also an internal spin canting (cation vacancy order−disorder) has to be taken into account to explain the magnetic properties of nanoparticles. The room-temperature coercive field decreases with decreasing crystallite size; however at low temperatures, the coercivity increases as the size decreases, reaching values larger than 3000 Oe. A model to explain the magnetic properties of these particles considering both surface and order−disorder effects is proposed.

Introduction

Magnetic particles with sizes in the nanometer scale are now of interest because of their many technological applications and unique magnetic properties which differ considerably from those of bulk materials. Magnetic ultrafine particles are applied in ferrofluids, refrigeration systems, etc, and they have potential applications to storage devices, medical imaging, and catalysis.[1−3]

The interesting magnetic properties of nanostructured materials are due to finite size effects and/or high surface/volume ratio, thus making the study of the interrelation between microstructure and magnetism very appealing. In this sense, very different magnetic properties have been observed with materials having similar grain sizes but produced by different methods[4−7] and, therefore, having different microstructures. As a consequence of that, there is a great variety of data in the literature about the properties of well-characterized γ-Fe_2O_3 nanoparticles.

For microcrystalline γ-Fe_2O_3 particles (particles of about 100 nm) it was found that the degree of order in the distribution of cation vacancies, inherent to the γ-Fe_2O_3 structure, affects the magnetic properties, suggesting that atom moments in the interior of the particle can significantly be influenced by canting effects.[8] Similar studies have been carried out in γ-Fe_2O_3 nanometer particles, and it was found that cation ordering takes place only in particles larger than 20 nm in diameter.[9] Therefore, the cationic disorder together with a magnetically disordered surface layer around the particles, proposed by various researchers as the particle size approachs the frontier of 10 nm,[10,11] could explain, at least in part, the reduction in saturation magnetization found at these sizes. The proposed effects are in many cases, however, obscured by a wide distribution of particle size and shape or by magnetic interactions between particles.

In this work we have studied the effect of size and structural ordering on the magnetic properties of γ-Fe_2O_3 nanoparticles (<20 nm) prepared by coprecipitation from solution and laser pyrolysis methods which provide samples with a narrow particle size distribution.[12,13]

* To whom correspondence should be addressed. Telephone: 34-1-334900. Fax: 34-1-3720623. E-mail: puerto@icmm.csic.es.

(1) Dormann, J. L., Fiorani, D., Eds. *Magnetic properties of fine particles*; Amsterdam: North-Holland, 1992.
(2) Awschalom, D. D.; DiVicenzo, D. P. *Phys. Today* **1995**, *4*, 43.
(3) Leslie-Pelecky, D. L.; Rieke, R. D. *Chem. Mater.* **1996**, *8*, 1770.
(4) Vollath, D.; Szabó, D. V.; Taylor, R. D.; Willis, J. O. *J. Mater. Res.* **1997**, *12*, 2175.
(5) Martinez, B.; Roig, A.; Obrador, X.; Molins, E.; Rouanet, A.; Monty, C. *J. Appl. Phys.* **1996**, *79*, 2580.
(6) Zang, Lei; Papaefthymiou, G. C.; Ying, J. Y. *J. Appl. Phys.* **1997**, *81*, 6892.
(7) Pascal, C.; Pascal, J. L.; Favier, F.; Elidrissi Moubtassim, M. L.; Payen, C. *Chem. Mater.* **1999**, *11*, 141.
(8) Morales, M. P.; Serna, C. J.; Bødker, F.; Mørup, S. *J. Phys.: Condens. Matter* **1997**, *9*, 5461.
(9) Haneda, K.; Morrish, A. H. *Solid State Commun.* **1977**, *22*, 779.
(10) Coey, J. M. D. *Phys. Rev. Lett.* **1971**, *27*, 1140.
(11) Martínez, B.; Obradors, X.; Balcells, Ll.; Rouanet, A.; Monty, C. *Phys. Rev. Lett.* **1998**, *80*, 181.
(12) Massart, R.; Cabuil, V. *J. Chim. Phys.* **1987**, *84*, 967.
(13) Veintemillas-Verdaguer, S.; Morales, M. P.; Serna, C. J. *Mater. Lett.* **1998**, *35*, 227.

10.1021/cm991018f CCC: $18.00
Published on Web 10/27/1999

Table 1. Description of the Sample Preparation Conditions for the Coprecipitated Samples

sample	base (1 M)	addition time (min)	temp (°C)
S−NH_4	NH_4(OH)	10	25
S−Na	Na(OH)	30	25
S−K	K(OH)	10	0
S−OH	K(OH) + 1% PVA	10	25

Material characterization in terms of particle size and shape was carried out by electron microscopy and X-ray diffraction. Additionally, infrared spectroscopy was used for the structural characterization regarding cationic order−disorder. The magnetic behavior of the samples was studied from the magnetization hysteresis loops and by Mössbauer spectroscopy at room temperature and 5 K.

Experimental Section

γ-Fe_2O_3 nanoparticles from 5 to 14 nm have been synthesized by coprecipitation of a mixture of the Fe(II) and Fe(III) salts in alkaline medium as described by other authors in detail.[12,14] The size of the particles can be controlled by the nature of the base used in the precipitation and the temperature[12] (Table 1). For this purpose, 50 mL of an aqueous solution 0.33 M in $FeCl_2$ and 0.66 M in $FeCl_3$ was added to 450 mL of 1 M basic aqueous solution under strong stirring. N_2 gas flow was previously passed through the basic solution to ensure that only magnetite was present in the final precipitate. Particles from 14 to 8 nm were obtained in this way and were called S−NH_4, S−Na, and S−K depending on the base used in the precipitation: NH_4(OH), Na(OH), or K(OH). The resulting black precipitate consisting of magnetite particles was decanted by magnetic settling, washed with distilled water, and dried. Then, γ-Fe_2O_3 particles were obtained by heating the magnetite at 250 °C for 2 h in air.

To obtain smaller particles, the iron salt mixture was added to a 1 M K(OH) solution with 1 wt % of poly(vinyl alcohol) (PVA) at room temperature following Lee et al.,[14] and the sample was called S−OH.

Particles smaller than 5 nm were synthesized by laser pyrolysis.[13] Thus, a dissolution of 30% $Fe(CO)_5$ in 2-propanol was nebulized by means of a ultrasound apparatus (15 W, 1.7 MHz) and the cloud formed partially dragged by the air stream (6 sccm). The mixture intersected a horizontal unfocused CO_2 laser beam (SYNRAD Duo-Lase model 57-2-208 W), operating at 82 W. The energy coupling of the laser to the reactant mixture is realized by the overlap of the laser wavelength (10.60 ± 0.05 μm) to the 2-propanol band at 10.50 ± 0.08 μm. The powder was collected by means of a stainless steel filter of 0.02 μm of pore size. The sample obtained under these conditions was named sample Fe23.

A decrease in the particle size was obtained by changing the pyrolysis experimental conditions. $Fe(CO)_5$ vapor was dragged by an ethylene stream of 6 sccm, the oxidation was induced by feeding the reaction chamber with a mixture of 220 sccm of Ar and 75 sccm of air and the laser power was 50 W. The evaporation temperature was about 22 °C and the sample named Fe4. Sample Fe4 was heated at 260 °C for 20 h to improve the crystallinity induced by this treatment (Fe4-260). A full description of the method producing different particle sizes will be the subject of a different publication.[15]

Particle size was determined from TEM micrographs in a 200 keV JEOL-2000 FXII microscope and X-ray line broadening analysis of the (311) reflection plane in a Philips 1710 powder diffractometer using Cu Kα radiation. For very broad diffraction lines (Fe4 and Fe4-260), a previous deconvolution of the signal in two components, the (220) and (311) reflections, was carried out in order to obtain a more accurate fwhm measurement. For the observation of the sample in the microscope, the particles were dispersed in acetone and a drop of the suspension was placed onto a copper grid covered by a perforated carbon film.

The microstructure of the samples was study by several techniques. X-ray diffraction performed between 10 and 30° (2θ) at 0.004° 2θ/s was used to determine the cationic ordering through the superlattice reflections which mainly appear in the low angle region. High-resolution electron microscopy (HREM) observations were carried in a Philips CM30 electron microscope operating at 300 kV. The images were Fourier filtered in order to minimize the contrast from the amorphous carbon support. Infrared spectra of the samples diluted in KBr at 1% were recorded between 850 and 250 cm^{-1} in a NICOLET 20SXC FTIR.

A conventional transmission Mössbauer spectrometer, operating in constant acceleration mode, with a ^{57}Co source in Rh was used to analyze the Fe valences as well as the nature of the iron oxide particles for the disordered samples. Spectra were recorded at room temperature, 80 and 4.2 K. The calibration was undertaken using a 25 μm thick α-Fe foil. The data were folded, plotted and fitted by a computer procedure using a single doublet for superparamagnetic samples and a doublet plus a distribution of hyperfine fields for the partially split spectra.

Magnetic properties of the samples were recorded in a vibrating sample magnetometer and a SQUID magnetometer (QUANTUM DESIGN MPMS-2). Saturation magnetization and coercivity were obtained from the hysteresis loops at room temperature and 5 K by applying magnetic fields of 1 and 5 T, respectively. The saturation magnetization was evaluated by extrapolating to infinite field the experimental results obtained in the field range where the magnetization increases, and it can be described by a $1/H$ law.

The magnetic particle size (D_{Mag}) was derived from the Langevin equation according to Chantrell et al.[16] In this equation, a log-normal distribution is used to describe the form of particle size distribution.[17] The magnetic particle diameter as well as the standard deviation can be derived from

$$D_{Mag} = \left[\frac{18kT}{\pi m_s}\sqrt{\frac{\chi_i}{3M_s}\frac{1}{H_0}}\right]^{1/3}; \quad \sigma = {}^1/_3\left[\ln\left(\frac{3\chi_i}{M_s}/\frac{1}{H_0}\right)\right]^{1/2}$$

where M_s and m_s are the saturation magnetization of the nanoparticles and the bulk phase, respectively. χ_i is the initial susceptibility calculated at low fields, in the region where the variation of M against H is linear and $1/H_0$ is obtained by extrapolating M to 0 at high fields, in the region where the relationship between M and $1/H$ is a straight line.

Results

Samples Characterization. In Figure 1 we show the morphological characteristics of some samples as observed by TEM. The particles are approximately isometric in shape and have a narrow particle size distribution (Table 2). For example, the average particle size calculated by counting 100 particles was 8 ± 2 nm for sample S−K. In the samples prepared from solutions, the average crystallite size, calculated from the (311) reflection using the Scherrer equation, agrees well with the size observed by TEM, suggesting that the particles are monocrystalline (Table 2). However, it should be noted that when the particles are very small, samples Fe4 and Fe4-260, the size calculated from X-ray gives lower values than those observed by TEM. Also,

(14) Lee, J.; Isobe, T.; Senna, M. *J. Colloid Interface Sci.* **1996**, *177*, 490.
(15) Morales, M. P.; Veintemillas-Verdaguer, S.; Serna, C. J. *J. Mater. Res.* **1998**, 14, 3066.
(16) Chantrell, R. W.; Popplewell, J.; Charles, S. W. *Physica* **1977**, *86−88B*, 1421.
(17) O'Grady, K.; Bradbury, A. *J. Magn. Magn. Mater.* **1983**, *39*, 91.

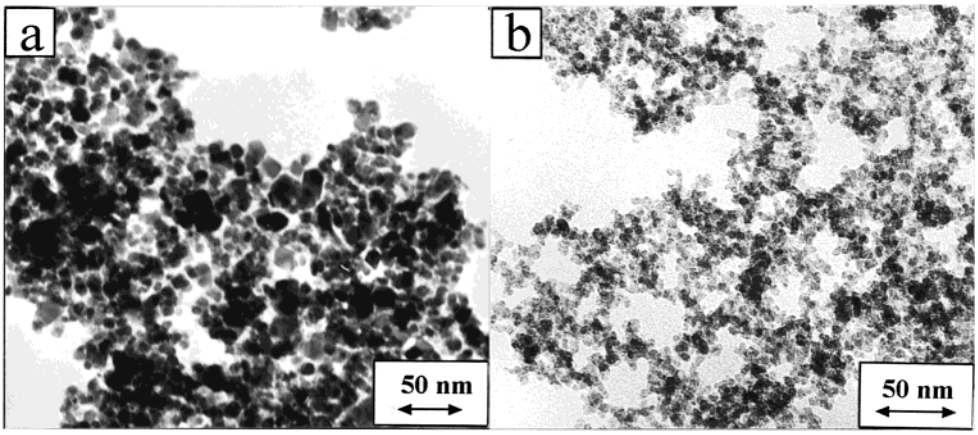

Figure 1. TEM micrographs of the γ-Fe_2O_3 nanoparticles prepared by different methods: (a) coprecipitation in solution, sample S−K; (b) laser pyrolysis, sample Fe4.

Table 2. Crystallite Size from X-ray Diffraction (D_{XR}), Particle Diameter from TEM (D_{TEM}) and Magnetic Size (D_{Mag}) and Magnetic Parameters for γ-Fe_2O_3 Nanoparticles[a]

					magnetic properties				
					RT			5K	
sample	preparation method		crystallite size (311) D_{XR} (nm)	particle size D_{TEM} (nm)	D_{Mag} (nm)	M_s (emu/g)	H_c (Oe)	M_s (emu/g)	H_c (Oe)
S−NH_4	co-precipitation	NH_4(OH)	13.5 (2)	12 (4)	7.3 (0.3)	69.6	29	77.3	260
S−Na		Na(OH)	10.3 (1)	9 (2)	6.9 (0.3)	62.3	8	71.9	350
S−K		K(OH)	8.9 (0.8)	8 (2)	6.6 (0.3)	54.8	5	60.9	414
S−OH		polyvinyl	4.8 (0.5)	4 (1)	5.1 (0.4)	40.3	0	47.0	469
Fe23	laser pyrolysis		5 (0.5)	5 (1)	5.7 (0.4)	29.5	0	35.7	700
Fe4-260			2 (0.5)	4 (1)	3.8 (0.5)	8.2	0	22.7	2100
Fe4			1 (0.5)	3.5 (1)	3.6 (0.5)	2.8	0	12.1	3000

[a] Measurement errors for the D_{XR} and standard deviations for the D_{TEM} and D_{Mag} are included in parentheses.

it should be taken into account that the error associated with the D_{XR} value is relatively higher for these samples due to the very broad peaks observed in the X-ray diffraction patterns (Figure 2). In general, from the D_{TEM} and D_{XR} values, a tendency can be inferred from sample S−NH_4 to sample Fe4, which shows not only a decrease in the particle size but also a decrease in the crystallinity.

X-ray diffraction patterns showed that maghemite constitutes the only crystalline phase present for all the samples with lattice parameters around 8.33−8.35 Å which was also corroborated by electron diffraction, in particular for the sample with lower crystallinity, Fe4 (Figure 3). HREM images of three different particles of sample Fe4 are displayed in this figure where lattice fringes characteristic of the maghemite structure were identified as (a) {220}, (b) {310}, and (c) {214} or {205}. The particles typically display good crystallinity although structural defects are occasionally found as that marked with an arrow in (c).

Mössbauer spectra were recorded for samples Fe-23, Fe4-260, and Fe4 (Figure 4). At room temperature, the spectra consist of a central doublet with an isomer shift of around 0.35 mm/s according to a superparamagnetic behavior of the particles. At 80 K the spectra clearly illustrate the particle size difference between the samples: $D_{Möss}^{Fe23} > D_{Möss}^{Fe4-260} > D_{Möss}^{Fe4}$ (Figure 4a). Hyperfine-fitted parameters are given in Table 3. The spectrum for sample Fe23 is almost totally split with a negligible quadrupole splitting and a mean field of 47.4 T (Figure 4a). An important fraction of particles are still unblocked at 80 K for samples Fe4-260 and Fe4, with average values of the hyperfine field of 39.2 and 28.4 T, respectively. However, at 4.2 K, the spectra for these two samples appeared to be completely split (Figure 4b). The best fit was obtained by fixing the vacancies in the octahedral positions and the relation $[Fe^{3+}]_{octahedric}/[Fe^{3+}]_{tetrahedric} \approx 1.67$, in agreement with stoichiometric γ-Fe_2O_3. On the other hand, no Fe^{2+} was detected in both samples. However, differences were found in relation to the hyperfine field values (Table 3 gives the mean field values) and line width, 0.82 and 0.86 mm/s for samples Fe4-260 and Fe4, respectively, corroborating the sample differences in particle size or/and crystallinity.

As expected, a progressive increase of the diffraction bandwidth is observed in the X-ray diffractograms as the particle size decreases (Figure 2). At the same time, the low angle superlattice reflections located between 10 and 30° (2θ), (110), (111), (210), and (211), can be clearly observed in sample S−NH_4 as well as in samples S−Na and S−K (Figure 2). Their intensity decreases with the particle size, and they disappear for samples with particle sizes smaller than 5 nm. The reflections (110), (210), and (211) are characteristics of a partial vacancy ordering within the maghemite structure[18] which gives rise to a primitive cubic lattice according to the space group $P4_132$. On the contrary, vacancy-disordered maghemite particles belong to the space group $Fd3m$, where the only allowed reflection at low angle is the (111), in accordance with a face-centered

(18) Morales, M. P.; Pecharroman, C.; González-Carreño, T.; Serna, C. J. *J. Solid State Chem.* **1994**, *108*, 158.

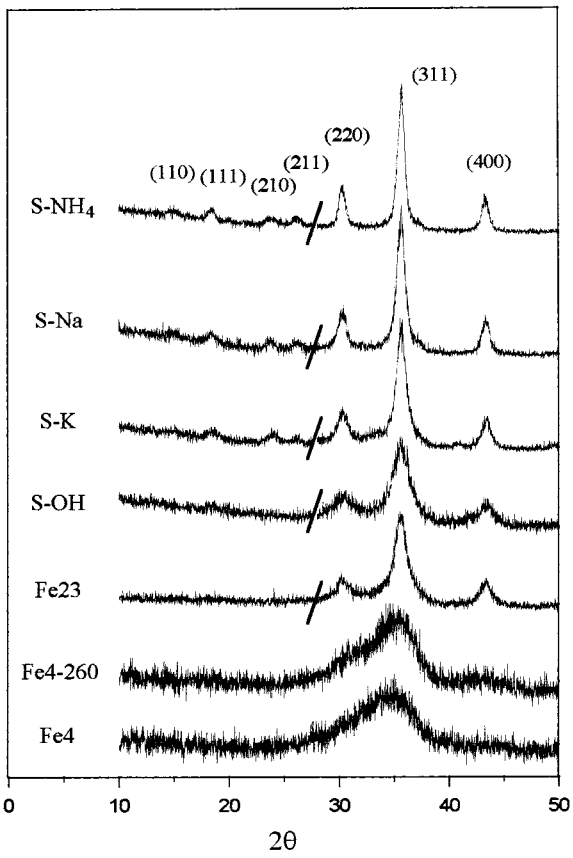

Figure 2. X-ray diffraction patterns for the γ-Fe_2O_3 nanoparticles prepared by coprecipitation in solution (S−NH_4, S−Na, S−K, and S−OH) and by laser pyrolysis (Fe23, Fe4-260, and Fe4). Patterns between 10 and 30° (2θ) were recorded at lower speed.

cubic lattice.[18] The smallest particles, where some vacancy order is observed, are 8 nm in diameter, much smaller than that previously reported of about 20 nm.[9] It is difficult to determine the reason for this discrepancy, but it could be due to the different particle preparation method, which is not well described in ref 9, or due to the detection limit of the X-ray measurement setup.

Further information concerning the vacancy distribution inside the particles was obtained by infrared spectroscopy, which has been previously shown to be very sensitive to the order−disorder characteristic of the maghemite structure.[18] The fact that γ-Fe_2O_3 nanoparticles approach an order−disorder transition at particle sizes close to 5 nm is illustrated by their infrared spectra (Figure 5). Thus, samples S−NH_4, S−Na, and S−K show the infrared features of a γ-Fe_2O_3 sample at least partially ordered, as evidenced by the multiple lattice absorption bands between 800 and 200 cm^{-1}. On the contrary, only two broad maxima at around 600 and 450 cm^{-1}, typical of disordered γ-Fe_2O_3,[18] are present for samples Fe4 and Fe4-260. It should be noticed that there is a slight increase in the intensity of the band at 600 cm^{-1} with respect to that at 450 cm^{-1} in sample Fe4-260, in agreement with an increase in the degree of order. A transition between both situations is manifested by samples Fe23 and S−OH, whose sizes are around 5 nm (Figure 5). Therefore, IR powder spectra show a progressive disorder in γ-Fe_2O_3 nanoparticles as the particle size decreases.

Magnetic Properties. Figure 6 shows the magnetization vs applied field for the samples at room temperature. It clearly illustrates the dependence of the magnetic properties on the particle size. Saturation magnetization, M_s, is almost reached for the largest particles at 10 kOe. An inset has been included in Figure 6 showing the hysteresis loops for the samples with the smallest particle sizes. In these samples, magnetization is still far from saturation.

In Table 2, the magnetic particle diameter (D_{Mag}) can be compared with the mean diameter of the particles obtained from electron microscopy (D_{TEM}). It can be seen that the magnetic size (D_{Mag}) is slightly smaller than the diameter obtained by TEM for the samples with larger particle size, while the agreement is quite good for the smallest particles. Several reasons can be outlined to justify these data. The method of magnetic particle size determination assumes the magnetization curve to be described by a Langevin function. Deviation from the Langevin function has been observed due to the presence of particle interactions and a particle size distribution.[16] These effects, especially the first, are expected to be more important for large particles with no superparamagnetic behavior up to much higher temperatures. Magnetic interactions between the particles should exist in all these samples since the particles have not been isolated in a matrix or fluid. However, in the case of the smallest samples, i.e., Fe4 and Fe4-260, a reduction in the interactions due to a lower value of M_s is expected[19] leading to a better

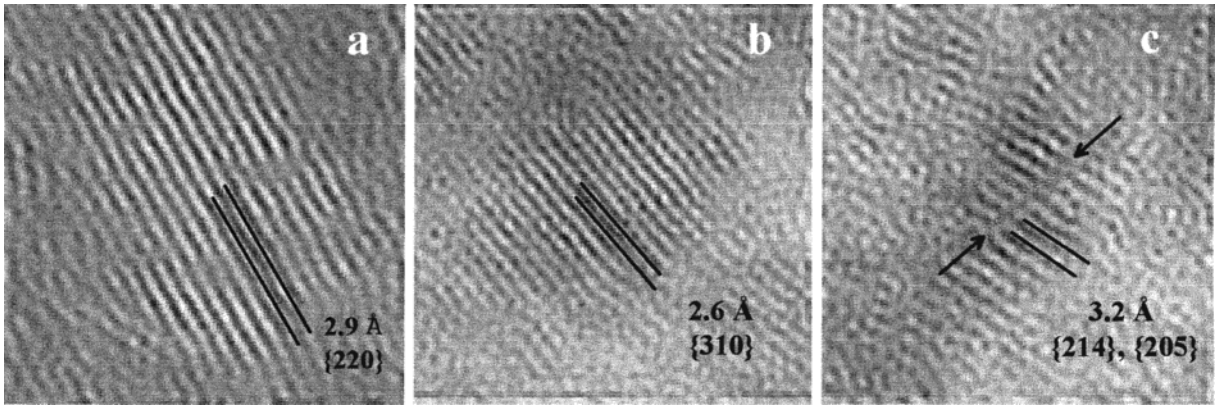

Figure 3. HREM images of three different particles displaying (a) {220}, (b) {310}, and (c) {214} or {205} lattice fringes characteristic of the maghemite structure.

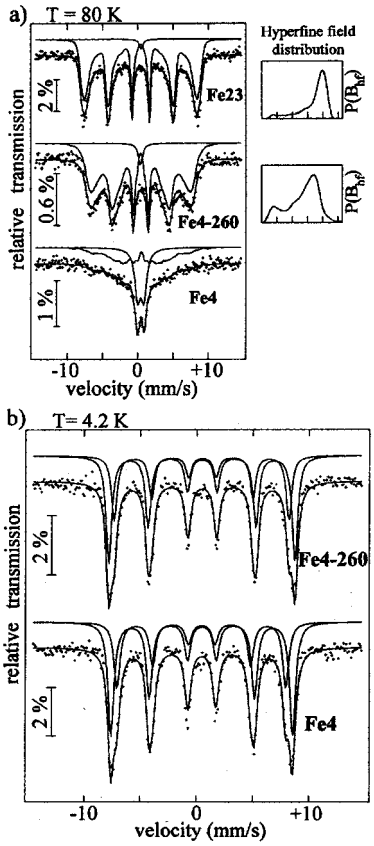

Figure 4. Mössbauer spectra: (a) at 80 K for samples Fe23, Fe4-260, and Fe4; (b) at 4.2 K for samples Fe4-260 and Fe4.

Table 3. Mössbauer Hyperfine Parameters for Nanometric Particles Prepared by Laser Pyrolysis at 80 and 4.2 K[b]

sample	temp (K)	isomer shift, δ[a] (mm/s)	quadrupolar splitting, ΔE_q (mm/s)	hyperfine field median value, $\langle B_{hf} \rangle$ (T)	area$_{subspectrum}$ (%)
Fe23	80	0.51 (1)	0.00 (1)		1.6
		0.44 (1)	0.00 (1)	47.4 (1)	98.4
Fe4-260	80	0.41 (1)	0.00 (1)	-	3.5
		0.46 (1)	0.00 (3)	39.2 (1)	96.5
Fe4	80	0.47 (1)	0.88 (1)	-	45.2
		0.51 (1)	−0.08 (2)	28.4 (1)	54.8
Fe4-260	4.2	0.48 (1)	−0.02 (1)	50.2 (1)	100
Fe4	4.2	0.48 (1)	0.01 (1)	48.9 (1)	100

[a] Referred to metallic iron. [b]Errors on the last digits are given within parentheses

agreement with the calculated magnetic size, which is very close to the size observed by TEM. In the case of the particles prepared by coprecipitation, the large discrepancies observed between D_{Mag} and D_{TEM} reflect not only the effect of stronger magnetic interactions but also the wider particle size distribution when compared with samples prepared by laser pyrolysis (Figure 1).

A plot of M_s vs particle size is shown is Figure 7. It is evident from the picture that, for samples with vacancy ordering, M_s decreases linearly with the particle size, leading to an extrapolation value of about 25 emu/g. Therefore, M_s values as small as those reported in some previous studies (5 emu/g)[4,11] are difficult to justify considering surface effects only. The existence of some

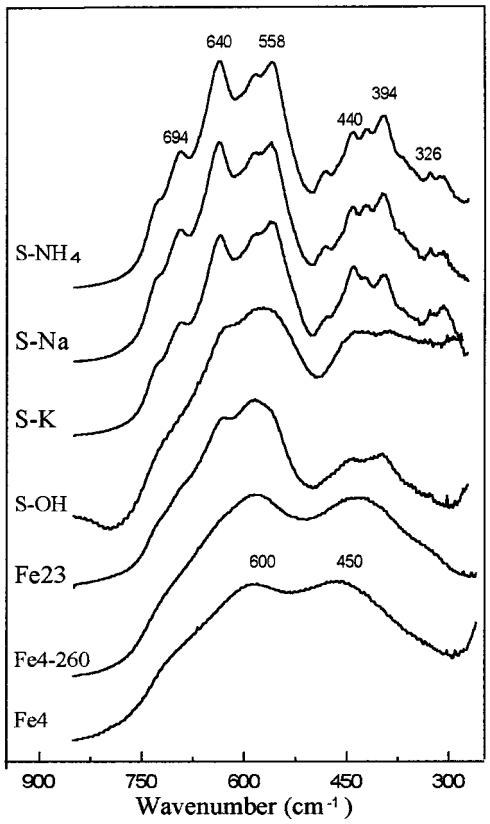

Figure 5. Infrared spectra for the γ-Fe_2O_3 nanoparticles prepared by coprecipitation in solution (S−NH_4, S−Na, S−K, and S−OH) and by laser pyrolysis (Fe23, Fe4-260, and Fe4).

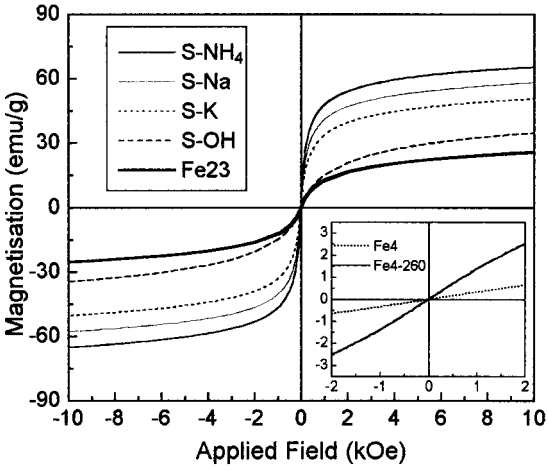

Figure 6. Hysteresis loops for γ-Fe_2O_3 nanoparticles at room temperature.

degree of spin canting in the whole volume of the particle, in addition to the disordered surface layer, could be an alternative explanation of this additional decrease of the saturation magnetization. In this sense we observe a strong decrease in the magnetization for particles smaller than 5 nm (about six cubic unit cells) only when the sample manifests vacancy disorder. Thus, it seems that, in addition to the surface effect, the order−disorder characteristic of the samples has also a strong influence on the final value of the saturation magnetization. It should be mentioned that similar evolution in the magnetization with the particle size has been found in γ-Fe_2O_3 nanoparticles prepared from micelles.[19] These results would explain, at least in part,

(19) Feltin, N.; Pileni, M. P. *Langmuir* **1997**, *13*, 3927.

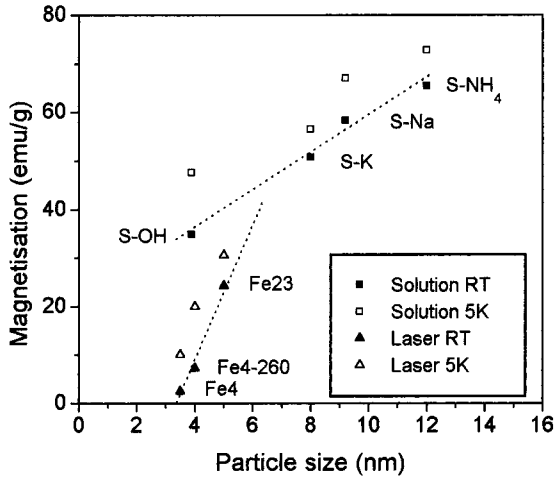

Figure 7. Variation of the saturation magnetization of the γ-Fe_2O_3 nanoparticles with particle size at room temperature and 5 K.

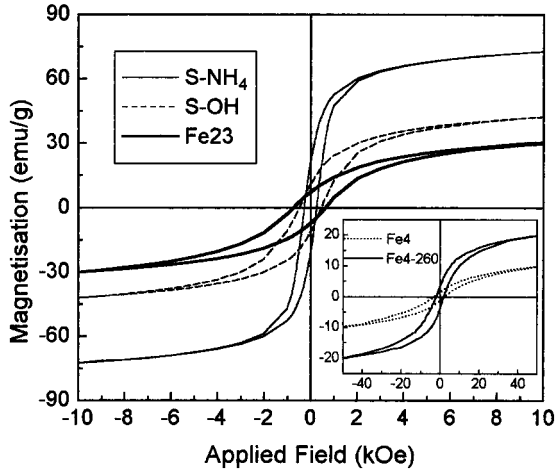

Figure 8. Hysteresis loops for γ-Fe_2O_3 nanoparticles at 5 K.

the different M_s values observed in samples with similar size as due to structural order−disorder differences, as well as the low M_s values reported for very small particles.

According to our results, superparamagnetic behavior at room temperature takes place only for particle sizes at which the particles show some vacancy disordered. At low temperature, 5 K, these samples show hysteresis loops characteristic of a superparamagnetic to ferrimagnetic transition (Figure 8). The high field irreversibility increases as the particle size decreases. For the smallest sample, Fe4, complete saturation is not reached even for fields of 55 kOe. This behavior is closely related with the existence of a magnetically disordered surface layer[11] in which direct competition of exchange interactions between surface spins takes place. Whether the origin of this magnetic disorder is related to the lack of crystallinity in the samples and/or the existence of some degree of cation vacancy disorder or is just a result of the reduced symmetry and uncompensated magnetic interactions of the surface spins is difficult to elucidate, and nowadays it is the subject of intense research.[20,21] Similar results have been previously observed in poorly

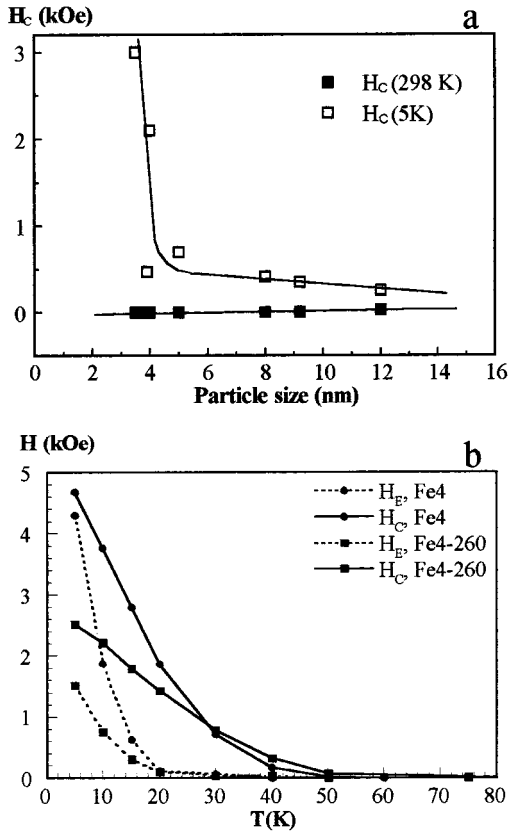

Figure 9. (a) Variation of the coercivity values of γ-Fe_2O_3 nanoparticles at room temperature and 5 K with particle size, within the nanometric range. (b) Temperature dependence of the coercive field H_c and the exchange anisotropy field H_E for the samples Fe4 and Fe4-260.

crystalline γ-Fe_2O_3 particles prepared by spray pyrolysis, which were not saturated even at 55 kOe.[22]

The low-temperature coercive fields H_c of the smallest samples, (Fe4 and Fe4-260), are very much larger than that expected (75 Oe) for coherent magnetization reversal of randomly oriented particles[23] thus, suggesting that the process is controlled by a different mechanism, whose strength is very much larger than that of magnetocrystalline anisotropy. The origin of these large values of H_c can be understood when comparing the values for samples with different particle size (Figure 9a). Again a striking increase is observed when the particles approach sizes smaller than around 5 nm. The temperature dependence of H_c for these two samples is also shown in Figure 9b. It is worth mentioning that the strong upturn of H_c takes place below about 40 K. This temperature corresponds to the appearance of the exchange anisotropy field H_E, also depicted in Figure 9b, which is defined as the field offset from the origin in the shifted hysteresis loops that appears after cooling the samples in a high magnetic field. The observation of this exchange anisotropy field is a clear indication of the existence of a magnetically disordered surface layer that becomes frozen below about 40 K.[11] Therefore, the observed increase of the coercivity can be attributed to

(20) Gangopadhyay, S.; Hadjipanayis, G. C.; Dale, B.; Sorensen, C. M.; Klabunde, K. J.; Papaefthymiou, V.; Kostikas, A. *Phys. Rev.* **1992**, *45*, 9778.

(21) Zang, D.; Klabunde, K. J.; Sorensen, C. M.; Hadjipanayis, G. C. *Phys. Rev.* **1998**, *58*, 14167.

(22) Martínez, B.; Roig, A.; Molins, E.; González-Carreño, T.; Serna, C. J. *J. Appl. Phys.* **1998**, *83*, 3256.

(23) Bates, G. In *Ferromagnetic Materials*; Wohlfarth, E. P., Ed.; North-Holland: 1980, 2, 442.

the extra energy required for the switching of the core spins that are pinned by the exchange interactions with the frozen spin glasslike surface layer. The direct competition of exchange interactions between surface spins lies at the origin of the observed high field irreversibility and accounts for the large experimental values of the coercive fields.

The relevance of the magnetically disordered surface layer on the magnetic properties becomes smaller as the particle size increases and eventually disappears for large enough particles. It is worth mentioning that, even X-ray diffraction data do not show traces of vacancy ordering in any of these two (Fe4, Fe4-260) samples, a clear increase of the saturation magnetization M_s, together with the concomitant decrease of both H_c and H_E, is observed after an annealing process at 260 °C with no substantial increase of the particle size (see Table 2). This observation is an indication of the influence of the crystallinity on the degree of the magnetic disorder.

Conclusions

It has been shown that vacancy order could be present in γ-Fe_2O_3 particles larger than 5 nm in diameter depending on the preparation method. This result represents a lower size limit between vacancy order−disorder structures than the one proposed in previous works (20 nm).[11] The fact that vacancy order exists down to such a small particle size may explain many experimental published data which seemed contradictory. The different saturation magnetization values reported in the bibliography for particles of similar sizes and particles larger than 5 nm can be justified by considering the different degree of vacancy ordering of the particles which is directly related to the sample preparation method. Even in the case of γ-Fe_2O_3 particles smaller than 5 nm, the unusually low values of M_s, as well as the large increase in coercivity found at low temperatures, may in part, be influenced by the different degree of structural vacancy order and crystallinity.

The large coercive fields observed for γ-Fe_2O_3 particles smaller than 5 nm seems to be in clear relation with the existence of a spin glasslike surface layer whose relevance on the magnetic properties of the whole particle becomes apparent when particle size is reduced beyond a threshold value. The unusual large values of H_c are explained taking into account the fact that core spins are pined by direct exchange interactions with the frozen spin glass surface layer. Thus, the increase of H_c is observed only below the freezing temperature of this disordered surface layer. Nevertheless, the existence of some degree of spin canting in the whole volume of the particle, due to different degrees of cationic vacancy disorder or crystallinity, responsible, in part, for the strong decrease of M_s and the dispersion of the values reported in the literature, should also be considered. Both effects, surface and order−disorder, are illustrated schematically for γ-Fe_2O_3 particles about 5 nm in diameter in Figure 10. The spinel structure of γ-Fe_2O_3 contains cation vacancies, which can be ordered, giving rise to a tetragonal superstructure, partially ordered, resulting in a cubic superstructure, or completely disordered with a high probability for the vacancies of being aggregated. Because of this internal disorder, some canting of core magnetic moments might occur, and this may be, in our opinion, partially responsible for the decrease in the saturation magnetization.

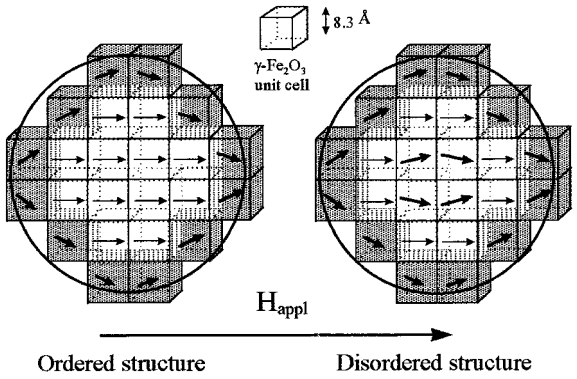

Figure 10. Schematic representation of the surface and order−disorder effects on the magnetic moments of a particle 5 nm in diameter in the presence of an applied magnetic field.

In summary, our results show that in order to properly understand the variation of the magnetic properties with particle size in the nanometric range, the surface canting as well as the order−disorder characteristic of the particles has to be taken into account.

Acknowledgment. The Spanish Commission for Science and Technology (CICYT) has supported this work under Project PB95-0002. Ll. Casas wishes to thank the "Generalitat de Catalunya" for his Ph.D. fellowship (1998-00055).

CM991018F